

Pressure induced atomic packing evolution and crystallization in $La_{75}Al_{25}$ metallic glass

Pingfei Deng(邓平飞), Suwan Wei(魏苏皖), Wangyang Ruan(阮王阳), and Min Wu(吴旻)
Citation: Chin. Phys. B, 2026, 35 (**5**): 058101. DOI: 10.1088/1674-1056/ae5174
http://cpb.iphy.ac.cn; http://iopscience.iop.org/cpb

What follows is a list of articles you may be interested in

Molecular dynamics study on the effect of cooling rate on the mechanical behavior of B2-CuZr enhanced bulk-metallic glass composites

Huahuai Shen(沈华淮), Kai Wang(王楷), Chenghao Chen(陈城豪), Jiaqing Wu(伍嘉卿), Mixun Zhu(朱谧询), Hongtao Zhong(钟泓涛), Yuanzheng Yang(杨元政), and Xiaoling Fu(付小玲)
Chin. Phys. B, 2025, 34 (**12**): 128102. DOI: 10.1088/1674-1056/adf9fa

Optimization of glass-forming ability and synergistic enhancement of strength plasticity in $Cu_{50}Zr_{46}Al_4$ metallic glasses through Ag additions

Dongmei Li(李冬梅), Zhongyi Zhang(张忠一), Bolin Shang(尚博林), Rui Feng(丰睿), Xuefeng Li(李雪枫), and Peng Yu(余鹏)
Chin. Phys. B, 2025, 34 (**8**): 086107. DOI: 10.1088/1674-1056/adcea1

Structural color of metallic glass through picosecond laser

Yue'e Zhang(张月娥), Xing Tong(童星), Yuqiang Yan(闫玉强), Shuo Cao(曹硕), Hai-Bo Ke(柯海波), and Wei-Hua Wang(汪卫华)
Chin. Phys. B, 2024, 33 (**10**): 108104. DOI: 10.1088/1674-1056/ad7672

Amorphous phase formation rules in high-entropy alloys

Qiu-Wei Xing(邢秋玮), Yong Zhang(张勇)
Chin. Phys. B, 2017, 26 (**1**): 018104. DOI: 10.1088/1674-1056/26/1/018104

Generalized model for laser-induced surface structure in metallic glass

Lin-Mao Ye(叶林茂), Zhen-Wei Wu(武振伟), Kai-Xin Liu(刘凯欣), Xiu-Zhang Tang(汤秀章), Xiang-Ming Xiong (熊向明)
Chin. Phys. B, 2016, 25 (**6**): 068104. DOI: 10.1088/1674-1056/25/6/068104

SPECIAL TOPIC — John Tse: Pioneer in high-pressure materials science

Pressure induced atomic packing evolution and crystallization in $La_{75}Al_{25}$ metallic glass

Pingfei Deng(邓平飞)[1,2,3], Suwan Wei(魏苏皖)[1,2,3], Wangyang Ruan(阮王阳)[1,2,3], and Min Wu(吴旻)[1,2,3,†]

[1] *College of Materials Science and Engineering, Zhejiang University of Technology, Hangzhou* 310014, *China*
[2] *Shaoxing Research Institute, Zhejiang University of Technology, Shaoxing* 312000, *China*
[3] *State Key Laboratory of Advanced Separation Membrane Materials, Hangzhou* 310014, *China*

(Received 4 February 2026; revised manuscript received 11 March 2026; accepted manuscript online 13 March 2026)

The pressure-induced structural transformation in metallic glass (MG) is a challenging and important subject in condensed matter physics. In the present first-principles molecular dynamics study, the atomic packing of $La_{75}Al_{25}$ MG under pressure was investigated, and the structure was predicted to crystallize at 92 GPa. It is found that the distributions of La and Al atoms are not homogeneous, as often assumed. In particular, Al atoms form aggregates in the glass structure, exhibiting strong covalent characteristics of the Al–Al bonds. The pressure-induced crystallization is not only caused by the dominant packing of the larger La atoms but is also facilitated by the presence of these rigid Al clusters.

Keywords: metallic glass, high pressure, molecular dynamics, first-principles

PACS: 81.05.Kf, 62.50.–p, 31.15.xv, 71.15.Mb

DOI: 10.1088/1674-1056/ae5174 **CSTR:** 32038.14.CPB.ae5174

1. Introduction

The structure–property relationship of metallic glasses (MGs) has been one of the most difficult problems in condensed matter science. Pressure can change the interactions between atoms and consequently alter the atomic packing and the properties of the material. It can therefore serve as a useful tool to further understand the underlying physics of MGs. Pressure-induced polymorphisms have been mainly found in oxide and sulfide glasses such as silica and ice.[1–5] Unlike these non-metallic glasses, which have covalent-bonded network structures and whose pressure-induced polymorphisms arise from the densification of the network structures and abrupt increases in atomic coordination, the structures of MGs, which are usually composed of metal atoms, were believed to be close-packed with non-directional metallic bonds and thus not likely to achieve further close packing upon compression.[6–9] However, several experimental works have shown pressure-induced polymorphisms in lanthanide-based MGs, and these polymorphisms are mainly caused by the delocalization of 4f orbitals in lanthanide elements at high pressure.[10,11] For instance, Sheng *et al.*[12] showed a pressure-induced low-density to high-density polymorphic transition in $Ce_{55}Al_{45}$ MG. From the synchrotron radiation x-ray Raman scattering (XRS) results of Zeng *et al.*[13] on $Ce_{75}Al_{25}$ MG, the pressure-induced polymorphism was proven to be related to 4f-orbital delocalization at 1.5–5 GPa. In our previous work, pressure-induced polymorphism was observed in main-group Ca–Al MG, and the polymorphism was suggested to originate from orbital hybridization between Ca 3d and Al 3p orbitals.[14] Very recently, a polymorphic transition was observed in a transition-metal-based MG under high pressure and was attributed to changes in bonding characteristics upon compression. Besides pressure-induced polymorphic transitions in MGs, pressure-induced amorphous-to-crystalline transitions observed in Ce–Al metallic glasses provide another perspective for understanding the microstructure evolution of MGs under pressure.[15] Zeng *et al.*[16] suggested that 4f-orbital delocalization eliminates the mismatch between the sizes of Ce and Al atoms and results in crystallization in $Ce_{75}Al_{25}$ MG, where the atomic sizes were determined from the close interatomic distances in the pair-correlation functions. On the other hand, our previous calculations suggested that crystallization is due to the dominant packing of the much larger Ce atoms, where the atomic sizes were defined as the volumes enclosed by zero-flux charge surfaces calculated from Bader analysis.[17] However, several critical problems remain to be solved. For instance, how can the major Ce atoms, with much larger atomic volumes, exhibit interatomic distances similar to those of Al atoms? How do the larger mismatch in atomic volume and the similar interatomic distances together contribute to crystallization?

In Ce–Al MGs, the contribution of 4f orbitals to crystallization remains under debate. Unfortunately, standard density functional theory (DFT) is not able to precisely describe localized 4f orbitals. The more sophisticated Hubbard + U method with a constant U value at different pressures is also

†Corresponding author. E-mail: wum@zjut.edu.cn

© 2026 Chinese Physical Society and IOP Publishing Ltd. All rights, including for text and data mining, AI training, and similar technologies, are reserved.

inappropriate, since the degree of orbital localization changes under pressure. La atoms have a similar electronic configuration to Ce atoms, except for the absence of a 4f electron. In this case, $La_{75}Al_{25}$ MG is an ideal system to study the atomic packing evolution from 0 GPa to high pressure and the possibility of pressure-induced crystallization, similar to that in $Ce_{75}Al_{25}$ MG. Sheng *et al.*[18] showed tunable atomic packing in $La_{75}Al_{25}$ MG under pressure up to 40 GPa, which is very close to the crystallization pressure of $Ce_{75}Al_{25}$ MG (38 GPa) reported in previous theoretical studies. Considering the larger bulk modulus of La (28 GPa) compared to Ce (22 GPa), the structure of $La_{75}Al_{25}$ MG over a wider pressure range should be investigated. In the present study, pressure-induced crystallization in $La_{75}Al_{25}$ MG is predicted to occur at 92 GPa, much higher than that of $Ce_{75}Al_{25}$ MG. The atomic cluster alignment analysis shows that the icosahedral short-range order (SRO) initially increases with pressure, indicating an increased degree of disorder. However, the icosahedral SRO starts to decay above 52 GPa, accompanied by an increase in face-centered cubic (fcc) SRO, which indicates a higher degree of structural order. These results not only reveal the mechanism of pressure-induced crystallization in these binary MGs but also provide further insight into the microstructure evolution upon compression.

2. Methods

First-principles molecular dynamics (FPMD) and electronic structure calculations were performed using the Vienna *ab initio* simulation package (VASP) based on density functional theory.[19,20] The effects of core electrons were described by the projector augmented wave (PAW) method.[21] The valence electronic configurations of $5s^25p^65d^16s^2$ and $3s^23p^1$ were used for La and Al, respectively. The Perdew–Burke–Ernzerhof (PBE) exchange–correlation functional was employed.[22] The wave functions were represented by a plane-wave basis set with an energy cutoff of 400 eV. The FPMD calculations were performed in the canonical ensemble (NVT),[23–25] and the Nosé–Hoover thermostat was used to control the temperature.[24] A single Γ point was used for Brillouin-zone sampling. To simulate the glass structure at ambient conditions, the La–Al supercell containing 108 atoms (81 La atoms and 27 Al atoms) was initially melted by heating to 2000 K, and the MD run lasted for at least 20 ps. The molten structure was then cooled stepwise to 300 K, with a cooling rate of $\sim 1.0 \times 10^{14}$ K/s. The La–Al glass structure at ambient conditions was obtained from an additional MD run at 300 K for at least 18 ps. High-pressure structures were obtained by isotropically reducing the supercell size step by step. At each pressure point, an MD run at 300 K was performed for at least 18 ps.

3. Results

In our previous first-principles calculations on $Ce_{75}Al_{25}$ MG, the employed procedure for generating glass structures under pressure was proven to reproduce the pressure-induced crystallization observed experimentally.[17] In the present work, in order to verify the validity of the theoretical method, the calculated structure factor and density at ambient pressure were compared with experimental results.[18] As shown in Fig. 1, the calculated structure factor is in good agreement with the experiment. Furthermore, the calculated density of 0.027 $Å^{-3}$ also agrees well with the experimental value.[18] This agreement indicates that the $La_{75}Al_{25}$ MG structures at ambient conditions and under compression are reasonable. The first main peak of the structure factor at 0 GPa is located at ~ 2.2 $Å^{-1}$, which is a general characteristic of MGs. Due to densification under compression, the first main peak shifts towards higher q with increasing pressure. In the previous study by Sheng *et al.*,[18] a shoulder developed on the higher-q side of the second peak with increasing pressure up to 40.2 GPa. The splitting of the second peak was attributed to the enhancement of icosahedral SRO. A similar development of the shoulder on the second peak is also observed in the present study. The intensity of the shoulder continuously increases up to 52 GPa (Fig. 1). Interestingly, the shoulder of the second peak begins to decrease when the pressure exceeds 52 GPa. In fact, the decay of the icosahedral SRO is expected, because icosahedral SRO lacks translational order and cannot fill space completely. At very high pressure (above 52 GPa in this case), the "glue" atoms located at interstitial sites between icosahedral clusters begin to interact more strongly with their neighbors, leading to deformation of the icosahedral clusters. Moreover, a shoulder on the lower-q side of the second peak develops at 92 GPa, indicating the emergence of a new short-range order distinct from icosahedral SRO. Upon annealing the structure at 800 K, the $La_{75}Al_{25}$ MG transforms into a crystalline phase, similar to the behavior of $Ce_{75}Al_{25}$ MG at 38 GPa reported in the previous study.[17]

The atomic cluster alignment (ACA) method was used to characterize the SRO.[26,27] In this method, clusters with nearest neighbors extracted from MD trajectories are aligned so that the SRO can be examined visually. This approach is more direct and intuitive compared with conventional structure characterization methods, such as cluster tessellation, which rely on the choice of a cutoff radius. The SROs obtained from ACA analysis of $La_{75}Al_{25}$ MG at selected pressures are shown in Fig. 2. Clearly, markedly different pressure-dependent SROs can be identified from both aligned clusters and their relative "energies". At 0 GPa, the aligned clusters show no clear SRO, indicating a highly disordered structure. With increasing pressure up to 52 GPa, the characteristics of icosahedral SRO become more pronounced. At 52 GPa, the relative "energy" of the icosahedral SRO is significantly lower than that of other

configurations, and the aligned clusters exhibit a clear icosahedral pattern. Consistent with the structure-factor results, the icosahedral SRO begins to deform above 52 GPa. At 68 GPa, although the fcc template has the lowest "energy", thermal annealing at 800 K does not lead to crystallization. When the pressure is further increased to 92 GPa, the fcc SRO becomes more dominant, with a lower "energy". Consequently, the glass structure transforms into a crystal upon thermal annealing at 800 K.

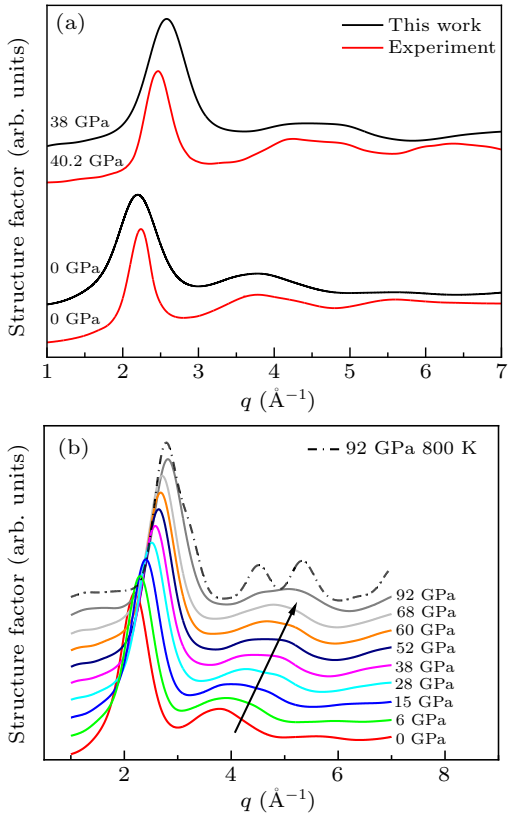


Fig. 1. (a) Comparison of the structure factors between theory and experiment for $La_{75}Al_{25}$ MG at ambient conditions and selected high pressures. (b) Pressure-dependent structure factors of $La_{75}Al_{25}$ MG in the present study.

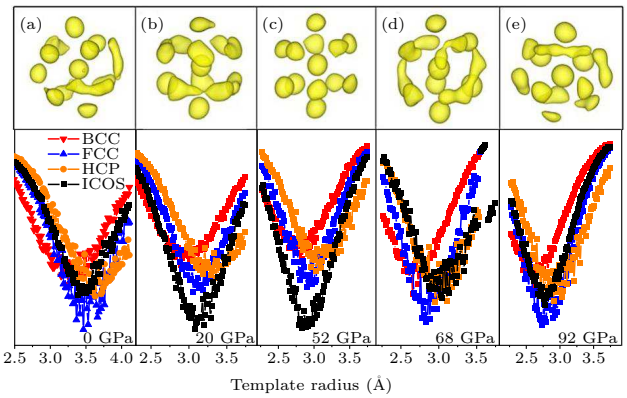


Fig. 2. Atomic cluster alignment analysis at selected pressures.

4. Discussion

To further investigate the pressure-induced structural evolution, the atomic pair-correlation function (PCF) analysis was performed, as shown in Fig. 3. The PCF of La–La exhibits a broad first peak at 0 GPa, consistent with the highly disordered structure at ambient pressure as discussed above. However, the first peak becomes significantly narrower at high pressure and approaches that of La–Al. The Al atoms are found to form aggregates in which the nearest Al–Al distance hardly shortens at high pressure. The bond distances obtained from the PCFs are often considered as a measure of atomic size and are consequently used to describe their contribution to structural changes. However, it is well accepted that the volume of a system is not linearly proportional to the cube of the nearest-neighbor distance in MGs. For instance, the bond-length ratio r_{La}/r_{Al} was found to decrease with increasing pressure in $La_{75}Al_{25}$ MG, whereas the charge distribution of crystalline La_3Al clearly shows that the size ratio V_{La}/V_{Al} increases with pressure (Fig. 4(a)). A similar discrepancy was also found in $Ce_{75}Al_{25}$ MG under pressure. Bader analysis, which defines atomic volumes based on zero-flux surfaces of the charge distribution, provides a more reliable description of atomic volume. Changes in Bader atomic charge and volume with pressure are shown in Fig. 4. The atomic volume fluctuation is quite large at 0 GPa, indicating that the structure is highly disordered. At high pressures, the SRO becomes more pronounced, and the fluctuation of atomic volumes becomes much smaller.

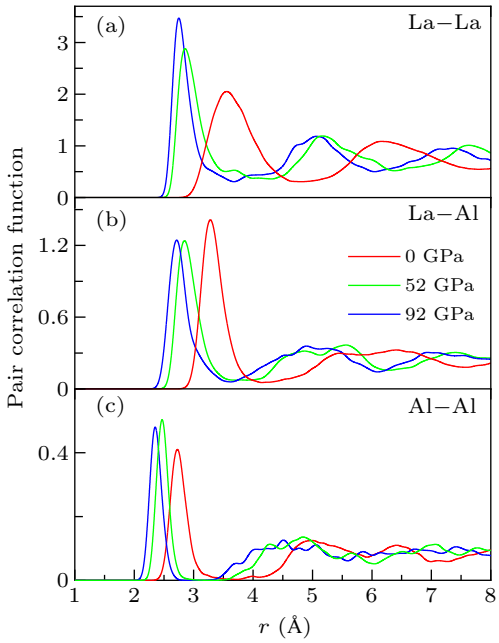


Fig. 3. Pair correlation functions of $La_{75}Al_{25}$ MG at selected pressures.

From the averaged Bader atomic volume and atomic charge, as shown in Figs. 4(d) and 4(e), each Al atom in the glass structure gains an average of 1.02 *e* from La atoms at 0 GPa. This is 0.2 *e* less than that in crystalline La_3Al and is likely due to the aggregation of Al atoms in the glass structure. Compared with $Ce_{75}Al_{25}$ MG, the charge transfer between La

and Al atoms in $La_{75}Al_{25}$ MG is larger due to the greater electronegativity difference between them. On the other hand, charge transfer reduces the atomic volume difference between La and Al at 0 GPa, resulting in a small volume ratio (V_{La}/V_{Al}) of 1.12. As pressure increases, the electronegativity difference is reduced, and Al atoms back-donate electrons to La atoms. The volume ratio V_{La}/V_{Al} continuously increases with pressure and reaches as high as 1.77 at 92 GPa, which is much larger than the V_{Ce}/V_{Al} value of 1.40 at 38 GPa when crystallization occurs. To explain the discrepancy between the large volume ratio and the short interatomic distances, the charge distribution and the electron localization function (ELF) of a selected layer in the crystallized $La_{75}Al_{25}$ structure are shown in Fig. 5. The volume plot shows that the average atomic volume of La is much larger than that of Al. However, no lattice site is occupied by multiple Al atoms, i.e., each Al atom occupies a distinct crystalline site despite its much smaller atomic volume. The electrons in the interstitial regions among La atoms behave like an electron gas, which is consistent with the low bulk modulus of pure La. Furthermore, locally, La atoms are close-packed, as reflected by the hexagonal charge distribution around La atoms. At higher pressure, the majority La atoms would form a close-packed crystal in the absence of Al atoms. At first glance, the atomic packing of the majority La atoms in $La_{75}Al_{25}$ MG appears to be a dominant driving force for crystallization. However, careful analysis of the glass structure reveals an unexpected feature: Al atoms in the aggregates are connected by localized electrons. These enhanced interactions result from the acceptance of itinerant electrons by Al 3p orbitals, leading to the strengthening of Al–Al covalent bonds. Such charge transfer has previously been

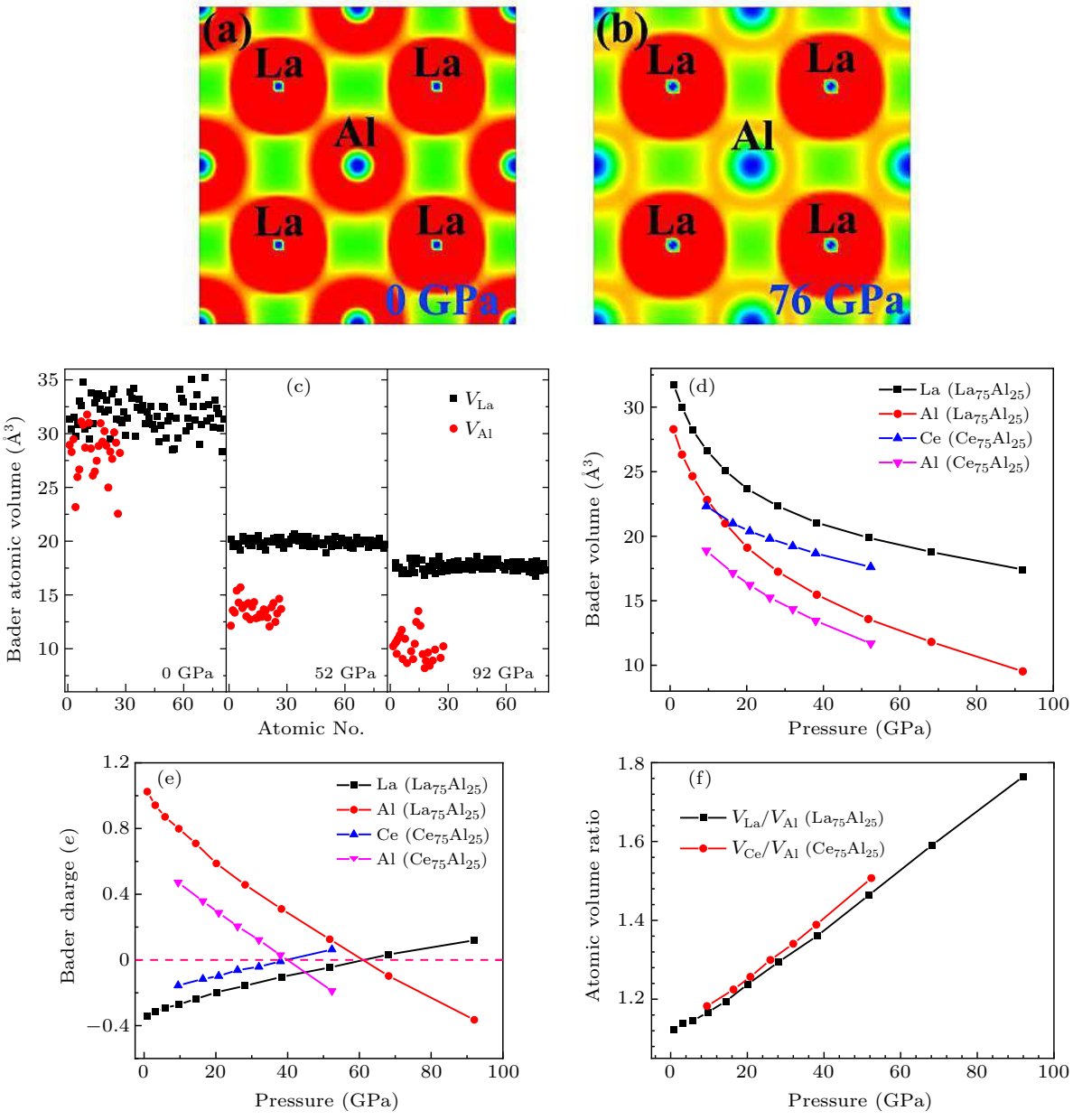


Fig. 4. (a) and (b) Charge distribution of crystalline La_3Al. (c)–(f) Bader volume and charge analysis.

shown to cause hardening in Li–Al alloys, where Li donates valence electrons to Al and strengthens Al–Al bonds.[28] This electron transfer can be rationalized by the significant difference in electronegativity between Al (1.61) and Li (0.98). In the present case, the electronegativity of La (1.1) is close to that of Li. In comparison, electron localization is much weaker between La and Al atoms. The large difference between La–Al and Al–Al interactions explains why the Bader atomic volume fluctuation of Al atoms is much larger than that of La atoms, even at 92 GPa. The presence of Al aggregates plays a vital role in promoting crystallization. To examine the detailed structural evolution during crystallization, a selected Al aggregate and its local structure are shown in Fig. 6. At 52 GPa, Al atoms are dispersed in the glass structure, which frustrates crystallization. When the pressure increases to 92 GPa, these Al atoms aggregate, with 1, 2, 4, and 5 Al atoms forming a planar structure that serves as a precursor to match the crystalline plane. After annealing at 800 K, the Al aggregate becomes more compact and matches well with La atoms to form a crystalline structure.

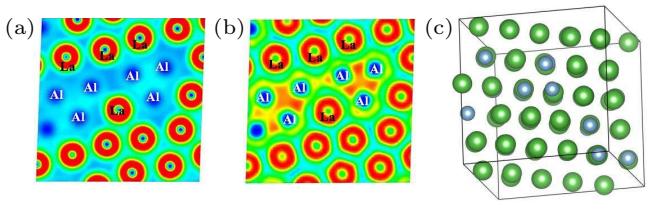


Fig. 5. (a) Charge distribution. (b) ELF of annealed $La_{75}Al_{25}$ at 92 GPa (ELF range: 0–0.8). (c) The crystalline structure of $La_{75}Al_{25}$ at 92 GPa.

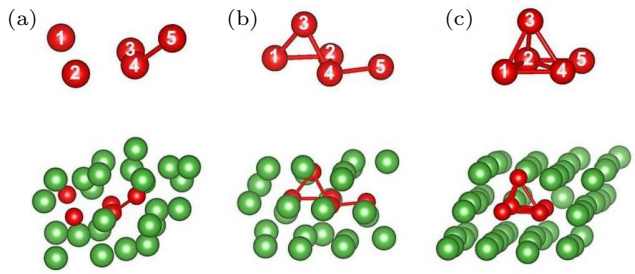


Fig. 6. Al aggregates and their local structures at selected conditions. (a) 52 GPa; (b) 92 GPa before annealing; (c) 92 GPa after annealing. The green and red spheres represent La and Al atoms, respectively.

5. Conclusion

In summary, first-principles MD calculations have been performed to investigate the evolution of atomic packing under pressure and to predict crystallization in $La_{75}Al_{25}$ MG. The incipient pressure-enhanced icosahedral SRO is reproduced, consistent with previous studies. Interestingly, the icosahedral SRO begins to decay when the pressure further increases above 52 GPa. When the pressure increases to 92 GPa, the atomic volume of La atoms becomes much larger than that of Al atoms. The dominant packing of larger La atoms, together with the role played by relatively rigid Al–Al bonds in Al aggregates, results in crystallization. The discrepancy between the large difference in atomic volume and the similar interatomic distances is thus resolved. Localized electrons between Al atoms maintain the Al–Al interatomic distances, compensating for the large volumetric mismatch with La atoms.

The theoretical analysis presented here offers new insights and a new paradigm for elucidating the behavior of MGs under compression.

Acknowledgment

This work was supported by the National Natural Science Foundation of China (Grant No. 51701180).

References

[1] Chen X J, Struzhkin V V, Song Y and Hemley R J 2008 *Proc. Natl. Acad. Sci.* **105** 20
[2] Yoo C S, Cynn H, Gygi F, Galli G, Iota V, Nicol M, Carlson S, Häusermann D and Mailhiot C 1999 *Phys. Rev. Lett.* **83** 5527
[3] Rueff J P, Kao C C, Struzhkin V V, Badro J, Shu J, Hemley R J and Mao H K 1999 *Phys. Rev. Lett.* **82** 3284
[4] Deb S K, Wilding M, Somayazulu M and McMillan P F 2001 *Nature* **414** 528
[5] Tulk C A, Hart R, Klug D D, Benmore C J and Neuefeind J 2006 *Phys. Rev. Lett.* **97** 115503
[6] Itie J P, Polian A, Galas G, Petiau J, Fontaine A and Tolentino H 1989 *Phys. Rev. Lett.* **63** 398
[7] Crichton W A, Mezouar M, Grande T, Stolen S and Grzechnik A 2001 *Nature* **414** 622
[8] McMillan P F, Wilson M, Daisenberger D and Machon D 2005 *Nat. Mater.* **4** 680
[9] Sheng H W, Luo W K, Alamgir F M, Bai J M and Ma E 2006 *Nature* **439** 419
[10] Li G, Wang Y Y, Liaw P K, Li Y C and Liu R P 2012 *Phys. Rev. Lett.* **109** 125501
[11] Zeng Q S, Struzhkin V V, Fang Y Z, Gao C X, Luo H B, Wang X D, Lathe C, Mao W L and Wu F M 2010 *Phys. Rev. B* **82** 054111
[12] Sheng H W, Liu H Z, Cheng Y Q, Wen J, Lee P L, Luo W K, Shastri S D and Ma E 2007 *Nat. Mater.* **6** 192
[13] Zeng Q S, Ding Y, Mao W L, Yang W, Sinogeikin S V, Shu J F, Mao H K and Jiang J Z 2010 *Phys. Rev. Lett.* **104** 105702
[14] Hafner J and Jaswal S S 1988 *Phys. Rev. B* **38** 7320
[15] Lou H B, Fang Y K, Zeng Q S, Lu Y H, Wang X D, Cao Q P, Yang K, Yu X H, Zheng L, Zhao Y D, Chu W S, Hu Z Y, Ahuja R and Jiang J Z 2012 *Sci. Rep.* **2** 376
[16] Zeng Q S, Li Y C, Feng C M and Jiang J Z 2007 *Proc. Natl. Acad. Sci. USA* **104** 13565
[17] Wu M, Tse J S, Wang S Y, Wang C Z and Jiang J Z 2015 *Nat. Commun.* **6** 6493
[18] Sheng H W, Ma E, Liu H Z and Wen J 2006 *Appl. Phys. Lett.* **88** 171906
[19] Kresse G and Hafner J 1994 *J. Phys. Condens. Matter* **6** 8245
[20] Kresse G and Joubert D 1999 *Phys. Rev. B* **59** 1758
[21] Blochl P E 1994 *Phys. Rev. B* **50** 17953
[22] Perdew J P, Burke K and Ernzerhof M 1996 *Phys. Rev. Lett.* **77** 3865
[23] Frenkel D, Smit B and Ratner M A 1997 *Phys. Today* **50** 66
[24] Car R and Parrinello M 1985 *Phys. Rev. Lett.* **55** 2471
[25] Truhlar D G 2010 *Phys. Today* **63** 54
[26] Fang X W, Wang C Z, Yao Y X, Ding Z J and Ho K M 2010 *Phys. Rev. B* **82** 184204
[27] Sun Y, Zhang F, Ye Z, Zhang Y, Fang X W, Ding Z J, Wang C Z, Mendelev M I, Ott R T, Kramer M J and Ho K M 2016 *Sci. Rep.* **6** 23734
[28] Rousseau R and Tse J S 1999 *Prog. Theor. Phys. Suppl.* **138** 47